DEVELOPMENT OF LIMB RADIATIVE TRANSFER MODELS FOR MARS REMOTE SENSING AND DATA ASSIMILATION.

J. Eluszkiewicz[1], G. Uymin[1], D. E. Flittner[2], J.-L. Moncet[1], E. Mlawer[1], and M. J. Wolff[3], *[1]Atmospheric and Environmental Research, Inc., 131 Hartwell Ave., Lexington, MA 02421, jel@aer.com, [2]NASA Langley Research Center, [3]Space Science Institute.*

Introduction: Measurements of the martian atmosphere are experiencing rapid growth. As on Earth, remote sensing from orbit offers the advantage of nearly continuous, global coverage and numerous instruments have been employed for this purpose, including Mars Orbiter Camera MOC, Mars Color Imager MARCI, Thermal Emission Spectrometer TES, Mars Climate Sounder MCS, Compact Reconnaissance Imaging Spectrometer for Mars CRISM, and Planetary Fourier Spectrometer PFS. MCS is a dedicated atmospheric instrument, while other instruments have yielded a wealth of information about the atmosphere in addition to their primary surface focus.
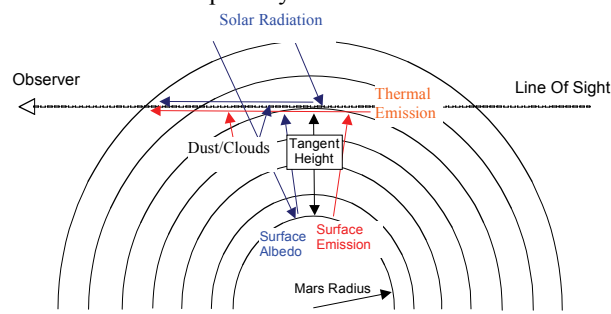

Figure 1: Limb-viewing geometry. Radiances measured by the observer come from the Sun (e.g., cameras, CRISM) or thermal emission (MCS, TES, PFS).

From the point of view of atmospheric studies, the dedicated limb-observing capability of the MCS and the recently selected ExoMars instruments, as well as the limb viewing "of opportunity" afforded by the TES, PFS, MOC, MARCI, and CRISM instruments offer significant advantages compared with the nadir-viewing mode. The geometry of limb measurements is illustrated in Figure 1. Chief among the advantages are the improved vertical resolution (particularly relevant to the studies of dynamic phenomena as reflected in the thermal structure) and the fact that observing against a cold space background (as opposed to a warm surface) offers the possibility of retrieving vertically resolved information about aerosols (including dust and H_2O and CO_2 ices) and minor gases (water vapor, carbon monoxide, methane, etc.). The main limitation to attaining the full scientific potential of limb measurements is the general lack of validated radiative transfer models. Such models must be capable, in a computationally efficient manner suitable for retrieval and radiance assimilation work, of accurately representing both gaseous absorption and aerosol scattering in a spherical geometry. The ubiquitous nature of aerosols in the martian atmosphere enhances the importance of scattering for limb viewing geometry (versus that of nadir).

Given the above considerations, we are developing rigorous radiative transfer models capable of simulating limb radiances in the presence of gaseous absorption and scattering. Our work has two overarching purposes. The first is to establish a set of rigorous benchmark calculations against which approximate methods to the limb absorption+scattering problem, such as employed in the operational MCS retrievals [1], can be validated. These calculations are carried out using a fully spherical radiative transfer model (RTM) for scattering and a line-by-line (LBL) model for gaseous absorption. The second objective is to develop a fast parameterization capable of accurately and efficiently calculating limb radiances in the presence of gaseous absorption and scattering using an approach designed to reproduce the accuracy of LBL calculations, but at a miniscule fraction of the computational cost.

Limb-Scattering Model: The scattering model employed in this project, the Gauss Seidel Spherical RTM (GSSRTM) [2, 3], has been in use for nearly 20 years. Scattering by molecules, dust, and clouds (with phase functions following Mie theory or any tabulated form) is computed. For the thermal-IR work described here, the polarization of scattered light is neglected with very little loss in accuracy, but with a significant reduction in run-time when compared to the polarized GSSRTM. The model is fully spherical (in the sense that all path lengths, including those for multiple scattering, are for a spherical atmosphere) and can be run in a line-by-line fashion over spectral features.

LBL Calculations of Gaseous Absorption: In both the benchmarking and parameterization portions of our work, an adaptation of AER's LBLRTM model [4] provides the line-by-line calculations of optical depths due to gaseous absorption. This adaptation, called P-LBLRTM, is appropriate for Martian atmospheric conditions (both present-day and paleo). A key issue in spectral radiative transfer calculations is line shape; this is already an issue for the current Earth

atmosphere, an environment for which a great deal is known about the impact of collisional line broadening, but is made even more acute when the dominant atmospheric constituent is not an 80/20 mixture of nitrogen and oxygen. Current spectroscopic databases such as HITRAN do not provide the parameters needed for modeling a broadening environment dominated by CO_2, for example, and our Earth-focused publicly available LBLRTM code does not allow for this possibility. We have rectified this in P-LBLRTM, redesigning the code and its input databases to permit the broadening effects of different gases to be taken into account (provided the pertinent parameters are available from quantum mechanical calculations and/or laboratory measurements). Completed upgrades to P-LBLRTM include: 1) Implementation of CO_2-broadened line parameters (half widths, line shifts, and temperature dependence of widths) for water vapor lines [5, 6], 2) Adjustment of the MT_CKD water vapor continuum model [4] to account for the difference between air- and CO_2-broadening of water vapor lines and their relative efficiency in generating collision-induced absorption, and 3) Incorporation of parameterization for the CO_2 collision-induced absorption [7]. Presently, we are incorporating parameters from Complex Robert-Bonamy calculations by R. Gamache that account for the temperature dependence of CO_2 self-broadened half widths and offer a substantial improvement over previous values [8]. In addition, we are upgrading the approach used to account for the shape of the far wings of CO_2 self-broadened lines via the implementation of the "chi-function" experimentally determined by Perrin and Hartmann [9]. P-LBLRTM and LBLRTM also have an implementation of the P and R branch line coupling for CO_2 [10]. Given existing uncertainties associated with radiation modeling in CO_2-dominated atmospheres, we welcome intercomparisons with other LBL models utilized for Mars atmospheric research.

Figure 2 shows monochromatic radiances computed using the P-LBLRTM+GSSRTM code, illustrating the kind of benchmark cases we aim to generate.

Fast RTM: "Brute force" monochromatic calculations of channel radiances are clearly impractical for operational applications. A standard approach to this problem is to develop a "fast" radiative transfer model. In our work, a fast RTM for a spherical scattering and absorbing atmosphere is being developed in two basic steps: 1) Reducing the LBL problem for gaseous absorption to a limited number of monochromatic calculations that reproduce the LBL calculations to within a pre-set accuracy, and 2) Performing scattering calculations at the selected monochromatic frequencies over a wide range of conditions. Step 1) consists in the mod-

eling using the Optimal Spectral Sampling (OSS) method [11], in which channel radiances are approximated as linear combinations of radiances computed at selected frequencies. This selection is accomplished in two stages, transmittance training and final selection, as described below. The OSS method treats gaseous absorption in a monochromatic way, making it a natural choice for coupling to a scattering code. The OSS spectral locations and their statistical weights are selected by comparing the resulting channel radiances against LBL calculations performed over a wide range of atmospheric profiles. These "training" profiles are chosen to be representative of the expected variability, including atmospheric temperature and composition, aerosol distribution and optical properties, surface pressure, surface emissivity and reflectivity, and viewing and solar angles. For this work, a training set of 150 profiles selected from the Mars Database v. 4.3 has been adopted.
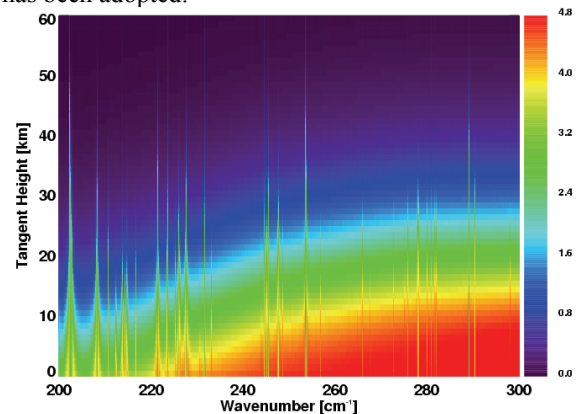

Figure 2: LBL radiances in the 230-260 cm^{-1} spectral range as a function of tangent height. Units are 100 x $W/m^2/cm^{-1}/sr$.

Transmittance Training. The high-resolution spectral element for transmittance training is a boxcar. The essence of the OSS approach in this case is to fit boxcar-averaged LBL clear-sky transmittances over a range of viewing angles (including horizontal paths) with their counterparts computed at selected nodes. The weights, or, coefficients, with which the nodes fit averaged transmittances, are then used to compute high-resolution *radiances* from the selected nodes only. This offers an obvious computational advantage: for a boxcar of 0.5 cm^{-1} width, the total number of LBL nodes is 2.5 x 10^4, whereas the OSS method utilizes ~5-10 nodes to achieve a desirable RMS accuracy (in this case, set to 10^{-4} in transmittance for each atmospheric path individually). For the MCS B3 channel, the total number of high-resolution boxcars is equal to 200 (covering the range 200-300 cm^{-1}), and the total number of selected monochromatic nodes is 1309. While the MCS B channels are not used in the current retrieval work [1], we adopted them for the

initial model development described herein because our spectroscopic upgrades described above are more complete at the present time in the far-IR than in the 15-μm region. The general approach we are implementing will be applicable to the MCS A channels as well. For a single CPU, running the GSSRTM code for 150 profiles for this number of nodes takes ~7.5 hours. As the output, we obtain limb radiances from 0 to 80 km altitude at 1-km resolution. It should be noted that the boxcar radiances and the associated OSS nodes and their weights are instrument-independent, streamlining the procedure for developing the model for different instruments. Applying the instrument channel filter function to the high-resolution boxcar radiances, we arrive at the set of channel radiances for a given instrument. Note that the computationally-intensive scattering calculations involved in this step are performed only at the selected nodes.

Final Selection. The final OSS selection is performed from the set of monochromatic nodes (in this example, 1309) pre-selected in transmittance training. The basic procedure is similar to that described for channel radiance training [11], performed simultaneously for all tangent heights, with some modifications due to orders-of-magnitude differences between radiances near the surface and at the top of the atmosphere. Also, the filter functions for the MCS B-channels depend on altitude. To address these issues and to minimize the number of selected OSS nodes, we performed OSS selection over a restricted range of altitudes, storing selected nodes and proceeding to the next altitude range with the existing nodes, and adding new ones, as necessary. The range of tangent heights for a single step of the final OSS selection was set to 5 km, reflecting the fact that the MCS B filter functions remain unchanged within this range. Two ways of selection have been explored: One starts from the surface towards the top of the atmosphere, while the other proceeds in the opposite direction. The first method yielded somewhat better results, in that the number of selected points was smaller for a given level of accuracy. Ultimately, we selected 27 monochromatic nodes, common for all tangent heights, but with the associated coefficients changing with tangent height. Preliminary estimates indicate that this number of nodes comes close to achieving the speed necessary for operational retrievals.

Validation. Validation is an integral part of our model development. In order to validate transmittance training, we compare boxcar radiances computed directly from line-by-line radiances with values computed at the pre-selected OSS nodes. Three profiles, selected from our set of 150 training profiles, have been considered in this task so far. Profile # 1 is

more typical than other two with respect to dust and ice clouds. Profile # 31 displays ice clouds located at lower altitudes, whereas profile # 110 has clouds at higher altitudes. Individual boxcar spectral regions adopted for validation are "opaque" or "transparent," as quantified by the number of selected OSS points. Representative results are shown in Figure 3 and Figure 4. On the left in these figures are shown profiles of limb radiances for altitudes from 0.5 to 79.5 km with a step of 1 km, while on the right are differences between the OSS-computed limb radiances and the reference calculations employing the brute-force P-LBLRTM+GSSRTM approach. Dashed red curves represent the nominal MCS noise level, set to 0.5% of the radiance value. The complete model will reflect the most recent information about noise and other instrument specs [1].
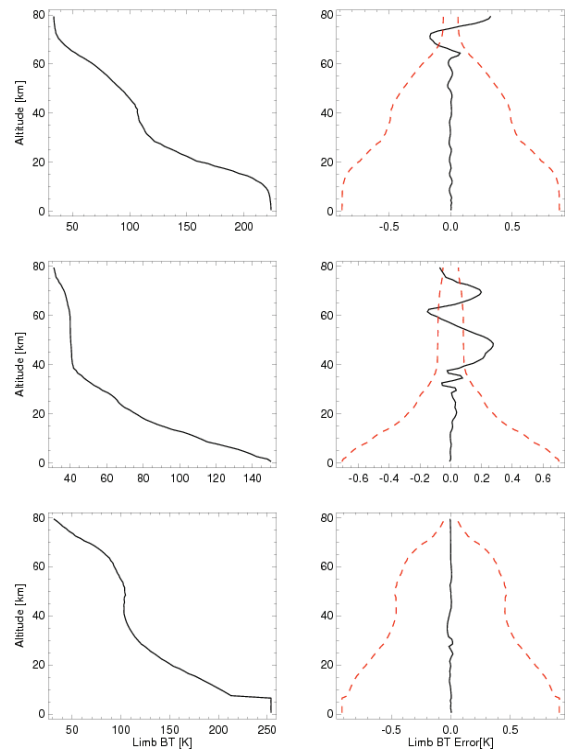

Figure 3: Radiances and OSS transmittance training errors for a boxcar at 202.25 cm^{-1} for three test profiles. This boxcar is opaque, with 13 OSS points. The red dashed lines on the right represent instrument noise, set to 0.5% of the radiance.

The final OSS selection is validated by computing full channel radiances (accounting for the relevant filter function), both in the line-by-line fashion and at the OSS nodes selected in the final stage. As shown in Figure 5 for the MCS B3 channel, the initial validation results are encouraging and we plan to continue our validation work as we proceed to develop the model for the MCS A channels used in the retrievals [1] and for other instruments.

References: [1] Kleinböhl et al. (2009) *J. Geophys. Res., 114,* E10006. [2] Herman B. M. et al. (1994) *Appl. Opt., 33,* 1760. [3] Herman B. M. et al. (1995) *Appl. Opt., 34,* 4563. [4] Clough S. A. et al. (2005) *JQSRT, 91,* 233. [5] R. Gamache (2008) personal comm. [6] Brown L. R. et al. (2007) *J. Mol. Spectrosc., 246,* 1. [7] Kasting, J. F. et al. (1984) *J. Atmos. Chem.*, 1, 403. [8] Yamamoto G. et al. (1969) *JQSRT, 9,* 371. [9] Perrin M. Y. and J. M. Hartman (1989), *JQSRT, 42,* 311. [10] Niro F. et al. (2005) *JQSRT, 95,* 469. [11] Moncet J.-L. et al. (2008) *J. Atmos. Sci. 65,* 3917.
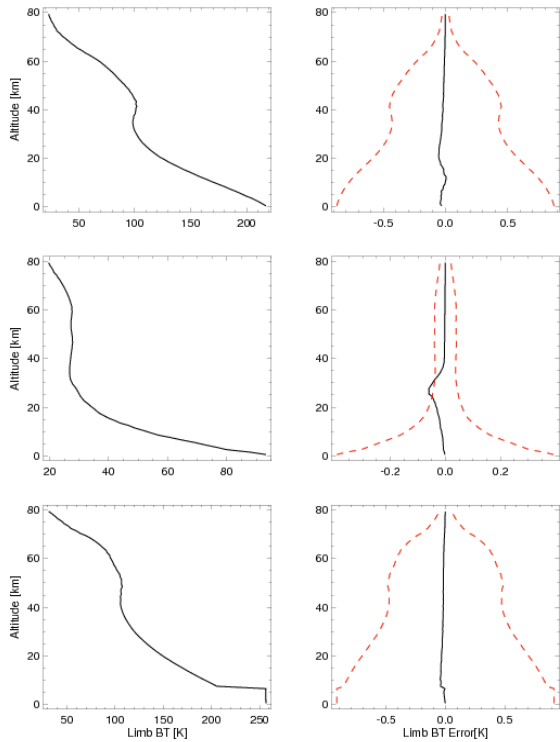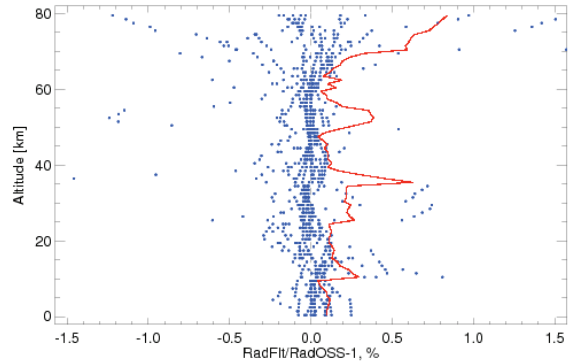

Figure 5: Blue dots: Differences between MCS B3 radiances computed monochromatically and by means of the OSS method for a set of 12 independent validation profiles. The RMS error for this set is plotted in red.

Figure 4: Similar to Figure 3, but for a transparent boxcar at 205.25 cm^{-1} (1 OSS point).